

Fast UV detection and hydrogen sensing by ZnO nanorod arrays grown on a flexible Kapton tape

J.J. HASSAN^{1,2*}, M.A. MAHDI^{1,2}, S.J. KASIM², NASER M. AHMED¹,
H. ABU. HASSAN¹, Z. HASSAN¹

¹Nano-Optoelectronics Research and Technology Laboratory (N.O.R.),
School of Physics Universiti Sains Malaysia, Penang 11800, Malaysia.

²Department of Physics, College of Science, University of Basrah, Basrah, Iraq.

ZnO nanorod arrays were grown on a flexible Kapton tape using microwave-assisted chemical bath deposition. High crystalline properties of the produced nanorods were proven by X-ray diffraction patterns and field emission scanning electron microscopy. Additionally, the photoluminescence spectrum showed higher UV peaks compared with visible peaks, which indicates that the ZnO nanorods had high quality and low number of defects. The metal-semiconductor-metal (MSM) configuration was used to fabricate UV and hydrogen gas detectors based on the ZnO nanorods grown on a flexible Kapton tape. Upon exposure to 395 nm UV light, the UV device exhibited fast response and decay times of 37 ms and 44 ms, respectively, at a bias voltage of 30 V. The relative sensitivities of the gas sensor made of the ZnO nanorod arrays, at hydrogen concentration of 2 %, at room temperature, 150 °C and 200 °C, are 0.42, 1.4 and 1.75 respectively.

Keywords: *fast response; UV detector; hydrogen gas sensor; ZnO nanorods; flexible Kapton tape*

© Wroclaw University of Technology.

1. Introduction

Interest in synthesis of nanomaterials on flexible substrates has been increasing in recent years [1]. Nowadays, one-dimensional nanostructured materials are one of the most significant nanostructure materials due to their properties and potential applications [2, 3]. Zinc oxide (ZnO) nanorods show potential in applications such as optoelectronics, gas sensing, field-emission (FE) [4], and UV detectors [5]. In these applications, the wide band gap (3.37 eV) and high binding energy (60 meV) at room temperature, massive surface-area-to-volume ratio, high sensitivity to oxygen adsorbed on the surface, efficient electric transport, and optical wave guiding are the key performance factors of ZnO nanorods [6–9]. ZnO nanorods possess ultraviolet (UV) and gas detection properties, which makes them suitable for fire detection, missile tracking, gas leakage detection, and environmental monitoring [7, 10]. Using flexible substrates

to grow ZnO nanorods offers benefits such as low cost and suitability for moving objects. In recent years, a growing number of studies have focused on enhancing response and recovery times by using different methods such as asymmetrical Schottky contact, selective growth of ZnO nanorods in the gap between interdigitated electrodes, and laterally aligned ZnO nanobridge arrays [11]. In this work, ZnO nanorod arrays were grown on a flexible Kapton tape to achieve fast response and recovery times for an UV detector, and good sensitivity for hydrogen gas sensing. To the best of our knowledge, several papers describing the lateral and vertical growth of ZnO nanorods on a flexible Kapton substrate, which have appeared in the literature, do not refer to developing UV detectors and gas sensors [12–16]. In this study, chemical bath deposition assisted by microwave irradiation was used to grow high-quality ZnO nanorods on a seeded, flexible Kapton tape. The UV detection and hydrogen gas sensing were carried out using the ZnO nanorod arrays grown on the flexible Kapton tape.

*E-mail: j1j2h72@yahoo.com; jalalj@ymail.com

2. Materials and methods

Kapton tape (50 μm), designed for the use in high temperatures and consisting of polyimide film and silicone adhesive [17], was used as a flexible substrate to grow ZnO nanorods. First, the Kapton tape was stacked on a glass substrate and cleaned several times by using 2-propanol and acetone to remove any contamination. After that, ZnO seed layer with a thickness of 100 nm was deposited using radio frequency (RF) sputtering at room temperature. To improve the seed layer quality, the substrate was placed on a hot plate for 2 h at 350 $^{\circ}\text{C}$ in air. Finally, the seeded substrate was inserted into the reaction vessel which contained solutions of zinc nitrate hexahydrate and hexamine of equal molarities (0.1 M). The vessel was heated to 90 $^{\circ}\text{C}$ in a microwave oven for 2 h. The prepared ZnO nanorod arrays were washed several times using 2-propanol and distilled water before annealing at 300 $^{\circ}\text{C}$ for 1 h [18, 19]. Fabrication of the metal-semiconductor-metal (MSM) UV and gas detector device was performed using RF sputtering of a Pt grid with the use of a shadow mask. The characterization of the ZnO nanorods was performed using X-ray diffraction (XRD) analysis (X'Pert Pro MRD PW3040; PANalytical, Almelo, the Netherlands), photoluminescence (PL) measurements (HR 800 UV; Horiba Jobin Yvon, Edison, NJ, USA), and field-emission

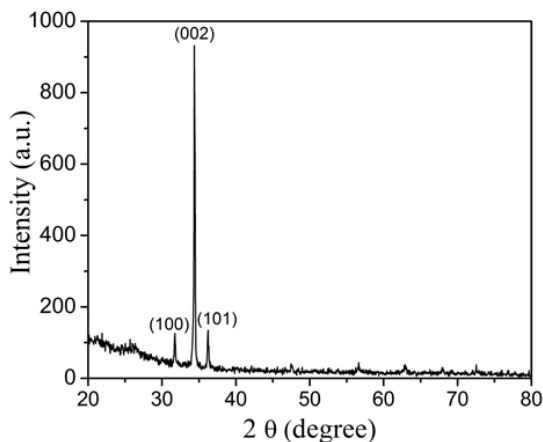


Figure 1. X-ray diffraction pattern of ZnO nanorod arrays grown on a flexible Kapton tape.

scanning electron microscopy (FESEM; FEI Nova nanoSEM 450). A current source (2400 SourceMeter, Keithley, Cleveland, Ohio, USA) that was connected to a PC was used to measure the electrical characteristics of the UV and gas-sensing device. The UV sensing was carried out by exposure to 395 nm UV LED, while the gas sensing was carried out at hydrogen concentration of 2 %.

3. Results and discussion

3.1. Characterization of the grown ZnO nanorod arrays

Crystal structure of the ZnO nanorod arrays was evaluated by using XRD. Fig. 1 shows a typical XRD pattern of the semi-vertically aligned ZnO nanorods that were grown on a Kapton tape. The XRD pattern shows the hexagonal (Wurtzite) structure of the ZnO nanorods with a high-intensity diffraction peak related to the (002) plane and the two low-intensity peaks related to (100) and (101) planes. All peaks corresponding to the ZnO phase can be indexed according to the ICDD diffraction data card (card no. 04-006-1673). The ZnO nanorods shown in FE-SEM image in Fig. 2 have a hexagonal structure and are aligned semi-vertically; their diameters range from 40 nm to 70 nm. The semi-vertically aligned ZnO nanorods make good contact between the neighboring nanorods in the space region between the two fingers contact, which offer short path to pass the electric current. The PL spectrum in Fig. 3 shows the high intensity UV peak located at 382 nm, which is due to the recombination of free excitons [20]. Intensity of this UV peak is much higher than that of the broad peak that is centered at 557 nm and is related to emission of deep-level defects [21]. This difference in intensities indicates that the grown ZnO nanorod arrays have a high quality with a few defects.

3.2. UV detection property

In dark ambient, the oxygen molecules chemisorbed on the surface of ZnO nanorod arrays create the depletion layer on the ZnO nanorods by collecting the electrons from the ZnO conduction

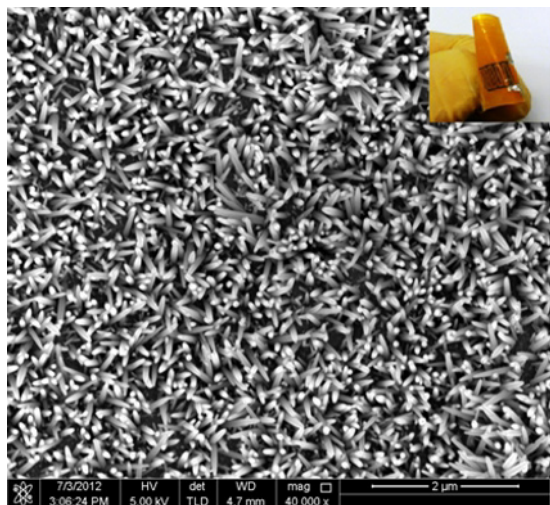


Figure 2. FE-SEM image of ZnO nanorod arrays grown on a flexible Kapton tape. The inset shows the photograph of ZnO nanorod arrays on the Kapton.

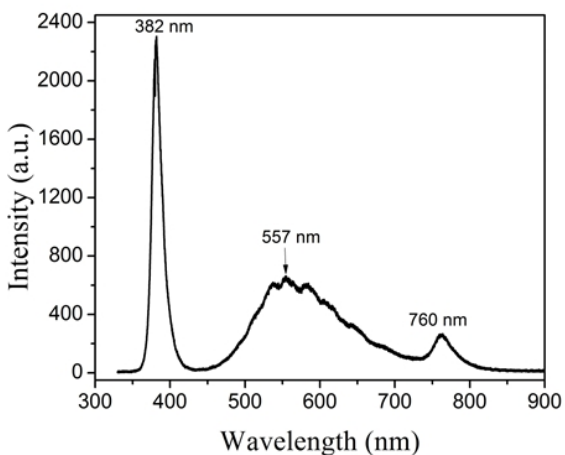


Figure 3. Room temperature photoluminescence spectrum of ZnO nanorod arrays grown on a flexible Kapton tape.

band ($\text{O}_2(\text{gas}) + e^- \rightarrow \text{O}_2^-(\text{ads})$). Upon UV illumination with the energy exceeding or equal to energy gap of the ZnO nanorod, the photo-induced electron-hole pairs will be generated ($h\nu \rightarrow e^- + h^+$).

Before the recombination between an electron and a hole, the holes migrate to the surface and naturalize the oxygen molecules $\text{O}_2^-(\text{ads})$, which enables the remaining free electrons to increase

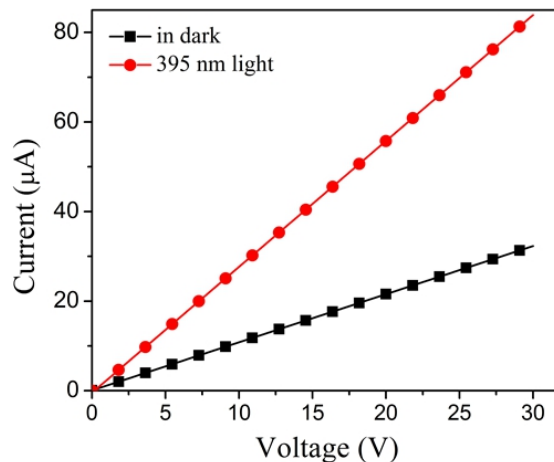


Figure 4. I – V characteristics of UV detector at dark and under 395 nm UV illumination.

the total current of the device ($h^+ + \text{O}_2^-(\text{ads}) \rightarrow \text{O}_2(\text{gas})$) [2, 11, 22].

Fig. 4 shows the typical I – V characteristics of ZnO nanorod arrays grown on Kapton tape in dark and under UV illumination (395 nm), which reveal an increase in photocurrent when illuminated by UV light. The on/off properties of the UV detector with an MSM structure were determined under 395 nm UV illumination. Fig. 5 (a – d) shows the corresponding increase in the photocurrent with increasing the bias voltage. In addition, repeatability of the UV detection was confirmed by repeating the on/off tuning 15 times (partially shown in Fig. 5(a – d)), and the results indicated acceptable variation with the time. The response time, which is defined as the time needed to reach the current value of $1 - 1/e$ of the maximum photocurrent, and the recovery time, which is defined as the time needed to reduce the current value to $1/e$ of the maximum photocurrent [23], were determined at bias voltages of 7, 10, 20, and 30 V. Faster response and recovery times compared with those in presented in literature [11] prove that the ZnO nanorods which were produced by subjecting a chemical solution to microwave heating had high structural quality. In addition, reduced transit time of carriers in low-diameter ZnO nanorods contributed to faster response and recovery times [24]. The fast recovery time can be attributed to the rapid recombination

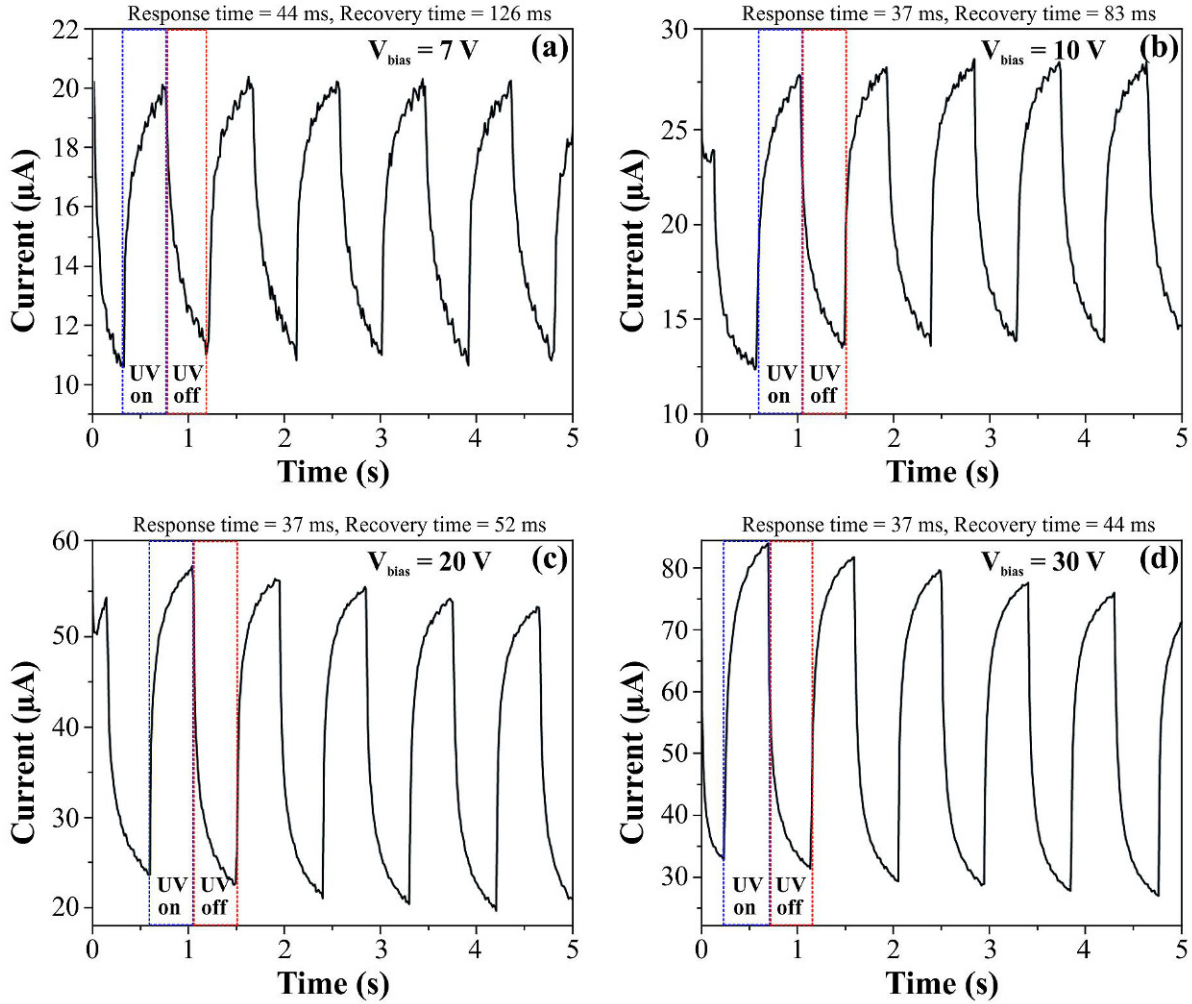


Figure 5. UV on/off photo-response of ZnO nanorod arrays grown on a Kapton tape under illumination with 395 nm light at different bias voltages.

processes of electron-hole pairs when the UV light is turned off [25].

The relative sensitivity shown in Fig. 5 was calculated for an UV detector at different bias voltages under on/off UV light exposure [26]:

$$S_{UV} = [(I_{UV} - I_{dark})/I_{dark}] \quad (1)$$

where I_{UV} is the current under UV exposure, and I_{dark} is the current in the dark. As presented in Table 1, when the bias voltage increases, the sensitivity increases and the decay time becomes faster because of the increase in electric field, which forces the carriers to collect at the finger contacts.

Table 1. Response and recovery times and sensitivity of UV detector at different bias voltages.

Bias voltage (V)	Response time (ms)	Recovery time (ms)	Sensitivity
7	44	126	0.83
10	37	83	1
20	37	52	1.5
30	37	44	1.8

3.3. Hydrogen gas sensing property

Upon exposure to hydrogen gas, the H_2 dissociates at the chemisorbed O_2 sites on the ZnO nanorod surface, which facilitates the interaction

between the resulting hydrogen atoms and the chemisorbed O_2 ions. This interaction increases the conductivity of ZnO nanorods by releasing the chemisorbed O_2 electrons to the ZnO conduction band [27–29]. The relative gas sensitivity of an electrochemical gas sensor represents the variation in the conductivity of the ZnO nanorods upon exposure to a hydrogen gas, which can be written in terms of the electric current passing via the nanorods, using the relationship [30]:

$$S_{gas} = [(I_{gas} - I_{air})/I_{air}] \quad (2)$$

where I_{gas} is the current passing in the ZnO nanorods measured at the presence of hydrogen gas, and I_{air} is the current passing in the ZnO nanorods measured in air. The sensitivity of the ZnO nanorod arrays grown on a flexible Kapton tape was measured at room temperature and at 150 and 200 °C. Fig. 6 shows the sensitivity of the gas sensor upon exposure to hydrogen gas at the concentration of 2 % in N_2 , followed by introducing air into the gas sensor chamber. The response and recovery times were calculated at 90 % and at 10 % of the sensitivity signal, respectively, and are equal to 400 s and 187 s at room temperature, and 339 s and 63 s at the temperature of 150 °C, and 320 s and 52 s at the temperature of 200 °C.

4. Conclusions

High-quality ZnO nanorod arrays were grown on a flexible Kapton tape by using microwave-assisted chemical bath deposition. The presence of high intensity UV peak compared with the visible broadband peak (related to the structural defects) of the photoluminescence spectrum indicate that the ZnO nanorods are of high quality. Photoconductive properties of an MSM UV sensor on the flexible Kapton tape were investigated, and faster response and recovery times compared with those obtained in the previous studies were achieved. High surface-area-to-volume ratio and high quality of ZnO nanorods are essential for shortening the response and recovery times of a UV sensor upon exposure to 395 nm UV light. The sensor made of ZnO nanorods grown on a flexible substrate have

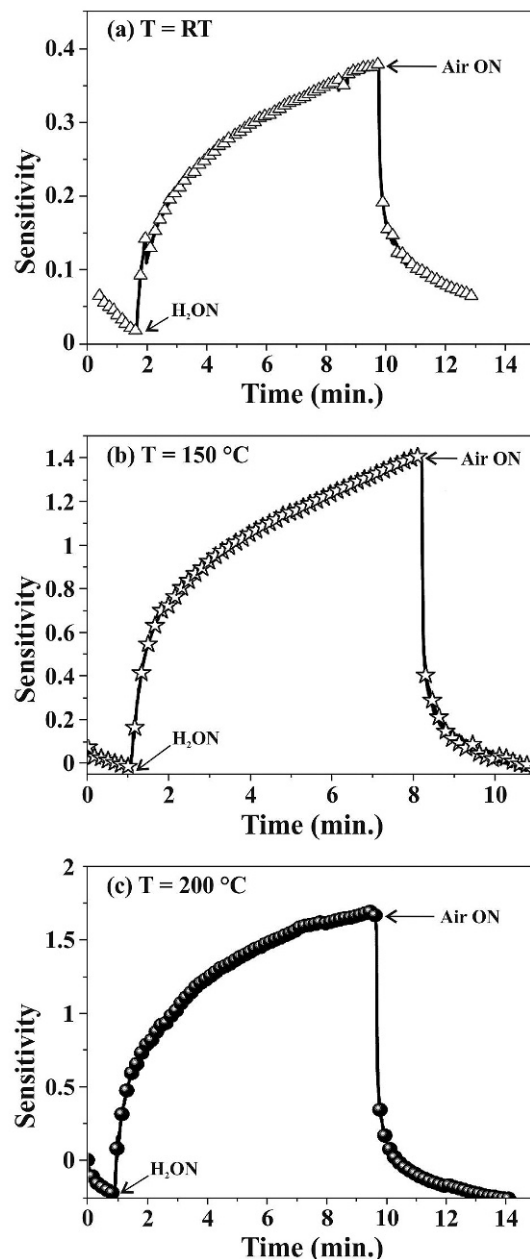


Figure 6. Gas sensitivity of ZnO nanorod arrays grown on a Kapton tape upon exposure to 2% H_2 at operating temperatures of (a) room temperature (b) 150 °C and (c) 200 °C.

excellent hydrogen sensing properties and can be easily inserted on a device with moving parts.

Acknowledgements

The authors gratefully acknowledge support from ERGS grant, and Universiti Sains Malaysia.

References

- [1] LIU J., WU W., BAI S., QIN Y., *ACS Appl. Mater. Interfaces*, 3 (2011), 4197.
- [2] ZHAI T., LI L., WANG X., FANG X., BANDO Y., GOLBERG D., *Adv. Funct. Mater.*, 20 (2010), 4233.
- [3] MAHDI M.A., HASSAN Z., NG S.S., HASSAN J.J., BAKHORI S.K.M., *Thin Solid Films*, 520 (2012) 3477 – 3484.
- [4] ZENG H., XU X., Y BANDO., GAUTAM U.K., ZHAI T., FANG X., LIU B., GOLBERG D., *Adv. Funct. Mater.*, 19 (2009) 3165 – 3172.
- [5] AKHAVAN O., MEHRABIAN M., MIRABBASZADEH K., AZIMIRAD R., *J. Phys. D:Appl. Phys.*, 42 (2009) 225305.
- [6] LIM M.A., LEE Y.W., HAN S.W., PARK I., *Nanotechnology*, 22 (2011) 035601.
- [7] SUN J., LIU F.-J., HUANG H.-Q., ZHAO J.-W., HU Z.-F., ZHANG X.-Q., WANG Y.-S., *Appl. Surf. Sci.*, 257 (2010) 921 – 924.
- [8] KAR J.P., DAS S.N., CHOI J.H., LEE T.I., SEO J., LEE T., MYOUNG J.M., *Appl. Surf. Sci.*, 257 (2011) 4973 – 4977.
- [9] WANG F., WANG C., CHEN J., YU Y., *Mater. Lett.*, 66 (2012) 270 – 272.
- [10] LIU K.W., MA J.G., ZHANG J.Y., LU Y.M., JIANG D.Y., LI B.H., ZHAO D.X., ZHANG Z.Z., YAO B., SHEN D.Z., *Solid-State Electron.*, 51 (2007) 757 – 761.
- [11] BAI S., WU W., QIN Y., CUI N., BAYERL D.J., WANG X., *Adv. Funct. Mater.*, 21 (2011) 4464 – 4469.
- [12] WEN L., WONG K.M., FANG Y., WU M., LEI Y., *J. Mater. Chem.*, 21 (2011) 7090.
- [13] QIN Y., YANG R., WANG Z. L., *J. Phys. Chem. C*, 112 (2008) 18734 – 18736.
- [14] WEINTRAUB B., DENG Y., WANG Z.L., *J. Phys. Chem. C*, 111 (2007) 10162 – 10165.
- [15] HONG J.I., J BAE., WANG Z.L., SNYDER R.L., *Nanotechnology*, 20 (2009) 085609.
- [16] ZHANG M.Y., NIAN Q., CHENG G.J., *Appl. Phys. Lett.*, 100 (2012) 151902.
- [17] Technical Data, http://www.tedpella.com/technote_html/16089-6-TN.pdf.
- [18] HASSAN J.J., HASSAN Z., ABU-HASSAN H., *J. Alloys Compd.*, 509 (2011) 6711 – 6719.
- [19] HASSAN J.J., MAHDI M.A., CHIN C.W., HASSAN Z., ABU-HASSAN H., *Appl. Surf. Sci.*, 258 (2012) 4467.
- [20] KANG D.-S., LEE H.S., S HAN.K., SRIVASTAVA V., BABU E.S., HONG S.-K., KIM M.-J., SONG J.-H., KIM H., KIM D., *J. Alloys Compd.*, 509 (2011) 5137 – 5141.
- [21] ZENG H., DUAN G., LI Y., YANG S., XU X., CAI W., *Adv. Funct. Mater.*, 20 (2010) 561 – 572.
- [22] CHAI G.Y., CHOW L., LUPAN O., RUSU E., STRATAN G.I., HEINRICH H., URSAKI V.V., TIGINYANU I.M., *Solid State Sci.*, 13 (2011) 1205 – 1210.
- [23] HU Y., ZHOU J., YE H.P.H., LI Z., WEI T.Y., WANG Z.L., *Adv. Mater.*, 22 (2010) 3327 – 3332.
- [24] BERA A., BASAK D., *Appl. Phys. Lett.*, 93 (2008) 053102.
- [25] LI Y., VALLE F. DELLA, SIMONNET M., YAMADA I., DELAUNAY J.-J., *Appl. Phys. Lett.*, 94 (2009) 023110.
- [26] MAHDI M.A., HASSAN J.J., NG S.S., HASSAN Z., AHMED N.M., *Physica E*, 44 (2012) 1716 – 1721.
- [27] LUPAN O., CHAI G., CHOW L., *Microelectron. Eng.*, 85 (2008) 2220 – 2225.
- [28] BASU A.D. S., *Mater. Chem. Phys.*, 47 (1997) 93 – 96.
- [29] HASSAN J. J., MAHDI M. A., CHIN C. W., ABU-HASSAN H., HASSAN Z., *J. Alloys Compd.*, 546 (2013) 107 – 111.
- [30] HASSAN J. J., MAHDI M. A., CHIN C. W., ABU-HASSAN H., HASSAN Z., *Physica E*, 46 (2012) 254 – 258.

Received 2012-09-28

Accepted 2012-12-31